Oxygen-Bound Heme−Heme Oxygenase Complex: Evidence for a Highly Bent Structure of the Coordinated Oxygen

Satoshi Takahashi,[†] Kazunobu Ishikawa,[‡] Noriko Takeuchi,[§] Masao Ikeda-Saito,[§] Tadashi Yoshida,[‡] and Denis L. Rousseau*,[†]

Contribution from AT&T Bell Laboratories, Murray Hill, New Jersey 07974, Department of Biochemistry, Yamagata University, School of Medicine, Yamagata 990-23, Japan, and Department of Physiology and Biophysics, Case Western Reserve University, School of Medicine, Cleveland, Ohio 44106-4970

Received August 8, 1994[⊗]

Abstract: Heme oxygenase is the first and rate limiting enzyme of the microsomal heme degradation pathway. Heme (iron protoporphyrin-IX), a co-factor and substrate of the enzyme, is catabolized through a process in which the key step involves the hydroxylation of the α-meso carbon of the porphyrin macrocycle by heme-bound oxygen. To study the mechanism of this reaction, we have formed the metastable O_2 adduct of the heme−heme oxygenase complex and observed that its resonance Raman spectrum displays an oxygen isotope shift pattern unlike those of any other O_2-bound heme proteins. Analysis of the spectra suggests that the Fe−O−O unit is highly bent, showing that steric interactions between the bound O_2 and the residues of the distal pocket result in a unique mechanism of oxygen activation. We propose that the terminal oxygen atom is in van der Waals contact with an α-meso carbon of the porphyrin ring.

Introduction

Heme oxygenase (HO), the first and rate limiting enzyme of the microsomal heme degradation pathway, captures iron protoporphyrin-IX (heme) and converts it into billiverdin-IXα, carbon monoxide, and free iron by using molecular oxygen and electrons donated by cytochrome P450 reductase.[1-4] Two isoforms of heme oxygenase designated as isoforms-1 and -2 have been isolated.[5,6] The physiological function of isoform-1, which is inducible by heme, is to digest hemes released from "old" hemoproteins.[1-4] Isoform-2, a constitutive enzyme mainly distributed in brain and testis, has been proposed to function as a generator of CO that serves as a neural messenger similar to nitric oxide.[4,7] Despite the difference in physiological function, the two isoforms have homologous secondary structures and spectroscopic properties, suggesting a similar catalytic mechanism.[6,8]

The enzyme, once complexed with its substrate heme, has optical absorption characteristic of myoglobin and hemoglobin.[5] Chemical and spectroscopic studies of the enzymatic turnover suggest that the enzyme opens the heme ring by three consecutive cycles of mono-oxygenation, each of which uses separate oxygen molecules axially coordinated to the heme-iron.[4,9] Therefore, the heme−HO complex has a reaction scheme analogous to cytochrome P450s; however, recent studies of the complex, which are enabled by the establishment of a bacterial expression system for the enzyme, demonstrated significant differences between the mechanism of oxygen activation by HO and by cytochrome P450s.[10] The resonance Raman and EPR studies showed that the axial ligand of the heme−HO complex is a neutral histidine, in contrast to the cysteine anion present in P450s.[11-13] This implies that the enzyme abandoned the vectorial polar environment across the heme which stabilizes the high oxidation state of the ferryloxo (Fe^{4+}=O) intermediate, the oxygen activated form of cytochrome P450s.[14] Furthermore, a ferryloxo form of the heme−HO complex, artificially made by adding a bulky peroxide to the ferric heme−HO complex, was shown to be incapable of cleaving heme.[15] It has been proposed that HO utilizes a ferric hydroperoxide (Fe^{3+}−OOH) intermediate as the oxygen activated form, giving the enzyme a unique mechanism of oxygen activation and suggesting unique

* Author to whom correspondence should be addressed: Tel. (908) 582-2609; Fax. (908) 582-2451; E-mail. dlr@physics.att.com.
† AT&T Bell Laboratories.
‡ Yamagata University.
§ Case Western Reserve University.
⊗ Abstract published in *Advance ACS Abstracts*, June 1, 1995.

(1) Tenhunen, R.; Marver, H. S.; Schmid, R. *J. Biol. Chem.* **1969**, *244*, 6388−6394.
(2) O'Carra, P. In *Porphyrins and Metaloporphyrins*; Smith, K. M., Ed.; Elsevier: Amsterdam, 1975; pp 123−153.
(3) Kikuchi, G.; Yoshida, T. *Mol. Cell. Biochem.* **1983**, *53/54*, 163−183.
(4) Maines, M. D. *FASEB J.* **1988**, *2*, 2557−2568.
(5) (a) Yoshida, T.; Kikuchi, G. *J. Biol. Chem.* **1978**, *253*, 4224−4229. (b) Yoshida, T.; Kikuchi, G. *J. Biol. Chem.* **1979**, *254*, 4487−4491.
(6) (a) Maines, M. D.; Trakshel, G. M.; Kutty, R. K. *J. Biol. Chem.* **1986**, *261*, 411−419. (b) Rotenberg, M. O.; Maines, M. D. *Arch. Biochem. Biophys.* **1991**, *290*, 336−344.
(7) (a) Verma, A.; Hirsch, D. J.; Glatt, C. E.; Ronnett, G. V.; Snyder, S. H. *Science* **1993**, *259*, 381−384. (b) Zhuo, M.; Small, S. A.; Kandel, E. R.; Hawkins, R. D. *Science* **1993**, *260*, 1946−1950. (c) Stevens, C. F.; Wang, Y. *Nature* **1993**, *364*, 147−149.
(8) Ishikawa, K.; Takeuchi, N.; Takahashi, S.; Matera, K. M.; Sato, M.; Rousseau, D. L.; Ikeda-Saito, M.; Yoshida, T. *J. Biol. Chem.* **1995**, *270*, 6345−6350.
(9) (a) Tenhunen, R.; Marver, H.; Pimstone, N. R.; Trager, W. F.; Cooper, D. Y.; Schmid, R. *Biochemistry* **1972**, *11*, 1716−1720. (b) Brown, S. B.; King, R. F. G. J. *Biochem. Soc. Trans.* **1976**, *4*, 197−201.
(10) (a) Ishikawa, K.; Sato, M.; Yoshida, T. *Eur. J. Biochem.* **1991**, *202*, 161−165. (b) Ishikawa, K.; Sato, M.; Ito, M.; Yoshida, T. *Biochem. Biophys. Res. Commun.* **1992**, *182*, 981−986.
(11) Sun, J.; Wilks, A.; Ortiz de Montellano, P. R.; Loher, T. M. *Biochemistry* **1993**, *32*, 14151−14157.
(12) Takahashi, S.; Wang, J.; Rousseau, D. L.; Ishikawa, K.; Yoshida, T.; Host, J. R.; Ikeda-Saito, M. *J. Biol. Chem.* **1994**, *269*, 1010−1014.
(13) Takahashi, S.; Wang, J.; Rousseau, D. L.; Ishikawa, K.; Yoshida, T.; Takeuchi, N.; Ikeda-Saito, M. *Biochemistry* **1994**, *33*, 5531−5538.
(14) (a) Ortiz de Montellano, P. R. In *Cytochrome P-450*; Ortiz de Montellano, P. R., Ed.; Plenum: New York, 1986; pp 217−271. (b) Poulos, T. L. *Adv. Inorg. Chem.* **1988**, *7*, 1−36. (c) Dawson, J. H. *Science* **1988**, *240*, 433−439.
(15) Wilks, A.; Ortiz de Montellano, P. R. *J. Biol. Chem.* **1993**, *268*, 22357−22362.

0002-7863/95/1517-6002$09.00/0

interactions between the bound oxygen and distal amino acids.[11,15,16]

The first cycle of the mono-oxygenation of the heme catalyzed by the enzyme has been postulated to proceed by reduction of the pseudostable O_2-bound complex to a hydroperoxide intermediate.[17] One of the axially coordinated oxygen atoms, presumably the terminal oxygen, then attacks the α-meso carbon of the porphyrin ring and hydroxylates it.[3,15] Therefore, the structure of the Fe−O_2 unit of the O_2-bound complex, a direct precursor of the oxygen-activated form, should sensitively reflect the distal interactions present in the activated complex. We have formed the $^{16}O_2$ adduct of the heme−HO complex and compared its resonance Raman spectrum to that of the $^{18}O_2$ adduct. The observed spectra show a unique isotope shift pattern unlike those of any other O_2-bound heme proteins. We interpret the spectra as evidence for a highly bent conformation of the Fe−O−O unit and further hypothesize that the α-meso carbon of the porphyrin ring is in van der Waals contact with the terminal oxygen.

Experimental Procedures

Truncated rat heme oxygenase isoform-1 protein, which was used for this study, was prepared by the procedure described elsewhere.[12,18] This catalytically active enzyme fragment is a water-soluble form of rat heme oxygenase-1, which lacks the hydrophobic C-terminal 26 amino acid sequence that anchors the enzyme to the microsomal membrane. The purified fragment was titrated with hemin until 90% complex formation. The complex was reduced by dithionite and loaded onto an anaerobic Sephadex G-25 column to remove extra reductant.[17] The concentration of the complex was adjusted to ca. 50 μM in 100 mM sodium phosphate (pH 7.4) or CHES (pH 9.0) buffers that contain 1 mM EDTA. Finally, $^{16}O_2$ or $^{18}O_2$ gas was added to the sample to form the oxy-form which was sealed in a Raman cell. To minimize the autooxidation of the O_2-bound complex, the sample solution was cooled immediately in ice and the Raman measurements were made as soon as possible. $^{18}O_2$ gas was purchased from ICON (Mt. Marion, NY). The 413-nm line of a krypton ion laser (Spectra Physics, Mountain View, CA) was used for Raman excitation. The power of the laser was set at ca. 20 mW at the sample. The sample cell was rotated at 1000 rpm and cooled by a stream of cold nitrogen gas during the Raman measurements. The Raman scattered light was dispersed by a single polychromator (Spex, Metuchen, NJ) and detected by a liquid nitrogen cooled CCD camera (Princeton Instruments, Princeton, NJ). A holographic filter (Kaiser, Ann Arbor, MI) was used to remove laser scattering. The noise spikes in the spectra caused by cosmic rays were removed by a standard software routine. No further data corrections were performed on the spectra, except for trace A of Figure 1 which was two-point base line corrected. The spectral slit width was set to about 5 cm^{-1}. The Raman shifts were calibrated by using indene as a standard. The accuracy of Raman shifts are about ±1 cm^{-1} for absolute shifts and less than ±0.25 cm^{-1} for relative shifts. The GF-matrix method was used for a simple three-body normal-mode analysis.[19] The following Urey−Bradley-type potential function was utilized.[20]

$$2V = K_1(\Delta r_{Fe-O_2})^2 + K_2(\Delta r_{OO})^2 + H(\Delta\delta_{FeOO})^2 + F(\Delta q_{Fe-O})^2$$

Where Δr_{Fe-O_2}, Δr_{OO}, $\Delta\delta_{FeOO}$, and Δq_{Fe-O} correspond to changes in the Fe−O and O−O bond distances, the Fe−O−O bending angle, and the Fe to terminal O nonbonding distance, respectively. The Fe−O stretching (K_1), O−O stretching (K_2), Fe−O−O bending (H), and Fe to terminal-O nonbonding interaction (F) force constants are chosen as K_1 = 3.15 mdyn/Å, K_2 = 5.1 mdyn·Å, H = 0.715 mdyn·Å, and F = 0.5 mdyn/Å, respectively, so as to reproduce the vibrational data for hemoglobin using structural parameters from X-ray crystallographic data (δ_{FeOO} = 155, r_{Fe-O_2} = 1.8 Å, and r_{O-O} = 1.2 Å).[21] The Raman data for hemoglobin (ν_{Fe-O_2} = 569.6 (for $^{16}O_2$)/545.4 (for $^{18}O_2$) cm^{-1}, δ_{FeOO} = 427/405 cm^{-1}) were re-examined to ensure the consistency of the shifts.[22-24] The shifts were the results of the average of the three independent measurements. The O−O stretching frequency (ν_{O-O} = 1130/1166 cm^{-1}) was adopted from ref 24. We also re-examined the Mb Raman data (ν_{Fe-O_2} = 571.4/544.8 cm^{-1}).[25]

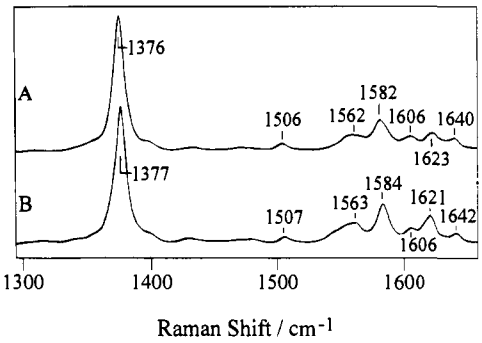

Figure 1. High-frequency resonance Raman spectra from the oxygen-bound form of the heme−HO complex and myoglobin. Trace A: Resonance Raman spectrum from the oxygen-coordinated heme−HO complex. The sample was dissolved in D_2O buffer (pD 7.4). The spectrum was a result of a 10-min data accumulation. A two-point linear base line correction were performed. Trace B: Resonance Raman spectrum from the oxygen-coordinated myoglobin. The sample was dissolved in H_2O buffer (pH 7.4). Other experimental conditions were the same as those of trace A.

Results and Discussion

The high-frequency resonance Raman scattering from the O_2-bound form of the heme-HO complex has a spectrum characteristic of other O_2-bound heme proteins. Traces A and B in Figure 1 correspond to the oxy-form of the heme−HO complex and myoglobin, respectively. The oxidation state maker line (ν_4) of the heme−HO complex appears at 1376 cm^{-1}, the same frequency (within 1 cm^{-1}) as that of oxymyoglobin, and indicates that the amount of electron donation between the coordinated oxygen and the porphyrin π-electron system is about the same in these two proteins. The spin and coordination state marker lines (ν_2 and ν_3) also demonstrate the similarity of the electronic states of the hemes in the heme−HO complex and myoglobin. However, the small differences in the frequencies and intensities of some of the lines may result from specific interactions between the bound O_2 and residues in the distal pocket that will be discussed below. It should be noted that the ν_3 line for the heme−HO complex appears at 1506 cm^{-1}, different from that of the ferric low-spin complex (1503 cm^{-1}), indicating that the amount of autoxidized (ferric) species in the sample solution is small.[11-13] There is no appreciable oxygen isotope sensitivity observed in this region.

In Figure 2, traces A and B show the low-frequency resonance Raman spectra of the $^{16}O_2$- and $^{18}O_2$-bound forms of the heme−

(16) Noguchi, M.; Yoshida, T.; Kikuchi, G. *J. Biochem. (Tokyo)* **1983**, *93*, 1027−1036.
(17) Yoshida, T.; Noguchi, M.; Kikuchi, G. *J. Biol. Chem.* **1980**, *255*, 4418−4420.
(18) Ito-Maki, M.; Ishikawa, K.; Mattera, M. K.; Sato, M.; Ikeda-Saito, M.; Yoshida, T. *Arch. Biochem. Biophys.* **1995**, *317*, 253−258.
(19) Wilson, E. B., Jr.; Decius, J. C.; Cross, P. C. *Molecular Vibrations*; McGraw-Hill: New York, 1955.
(20) Nagai, M.; Yoneyama, Y.; Kitagawa, T. *Biochemistry* **1991**, *30*, 6495−6503.
(21) (a) Shaanan, B. *Nature* **1982**, *296*, 683−684. (b) Shaanan, B. *J. Mol. Biol.* **1983**, *171*, 31−59.
(22) Brunner, H. *Naturwissenschaften* **1974**, *61*, 129.
(23) Jeyarajah, S.; Proniewicz, L. M.; Broder, H.; Kincaid, J. R. *J. Biol. Chem.* **1994**, *269*, 31047−31050.
(24) Hirota, S.; Ogura, T.; Appelman, E. H.; Shinzawa-Itoh, K.; Yoshikawa, S.; Kitagawa, T. *J. Am. Chem. Soc.* **1994**, *116*, 10564−10570.
(25) Tsubaki, M.; Yu, N.-T. *Proc. Natl. Acad. Sci. U.S.A.* **1981**, *78*, 3581−3585.

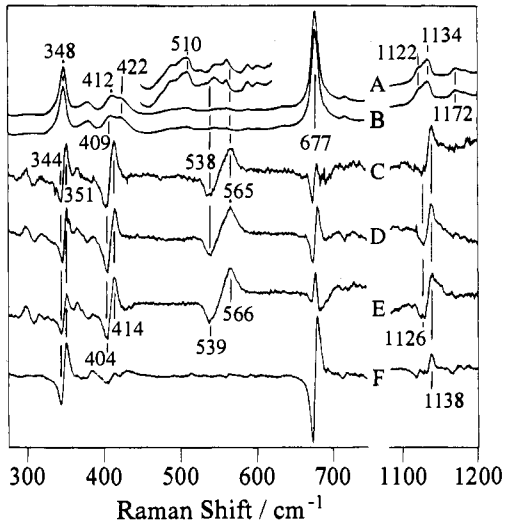

Figure 2. Low-frequency resonance Raman spectra from the oxygen-bound form of the heme−HO complex. Trace A: Resonance Raman spectrum from the $^{16}O_2$-coordinated heme−HO complex at pH 7.4 and at ca. 5 °C. The spectrum was a result of a 20-min data accumulation. Trace B: Same as trace A but the sample was coordinated by $^{18}O_2$. The five times expanded spectra of traces A and B in the 450−600-cm^{-1} region are also indicated above trace A in the corresponding order. Trace C: The difference spectrum between traces A and B. The scale of trace C is about 20 times larger than that of traces A and B. Trace D: Same difference spectrum as trace C but the samples were at pH 9.0. Trace E: Same difference spectrum as trace C but the samples were in buffered D_2O. Trace F: The derivative pattern of trace A. The spectrum was calculated by shifting the spectrum in trace A to lower frequency by 0.25 cm^{-1} and subtracting it from the original trace. The intensity scale was set to be the same as that of trace C.

HO complex. Their difference spectrum is shown in trace C, which reveals several oxygen isotope sensitive lines. The largest isotope shift (27 cm^{-1}) is in the line at 565 cm^{-1} for the $^{16}O_2$ adduct. Based on the frequency of this line and its isotope shift, we assign it as the Fe−O_2 stretching (ν_{Fe-O_2}) mode of an O_2 adduct of the heme−HO complex.[26] The frequency of the ν_{Fe-O_2} mode is the lowest among O_2-coordinated heme proteins having neutral histidine as a trans ligand.[22,25-27] The intensity of the stretching mode (measured as a peak to trough intensity difference in trace C) compared to that of the ν_7 mode at 677 cm^{-1} is about 3%, which is smaller than those of oxymyoglobin (ca. 7%) and hemoglobin (ca. 10%).

The oxygen isotope difference spectrum in the region below 450 cm^{-1} is complicated: the lines at 414 and 351 cm^{-1} which are as intense as the ν_{Fe-O_2} mode have peak to trough shifts of 10 and 7 cm^{-1}, respectively, and weaker but reproducible shifts of other lines between 280 and 400 cm^{-1} are seen. There is also a small isotope shift observed at 1138 cm^{-1}. That all the observed shifts are from the same oxygen-bound species is confirmed by a series of spectra taken under different experimental conditions at ~5 °C: C, pH 7.4; D, pH 9.0; E, (D_2O) pD 7.4—all of which have the same oxygen−isotope difference spectra. Figure 3 is an enlargement of the spectra shown in Figure 2 and confirms the identity of the shift pattern in the region lower than 450 cm^{-1} for various experimental conditions. Spectra taken at room temperature or spectra taken immediately after the dioxygen coordination or 30 min later also all show

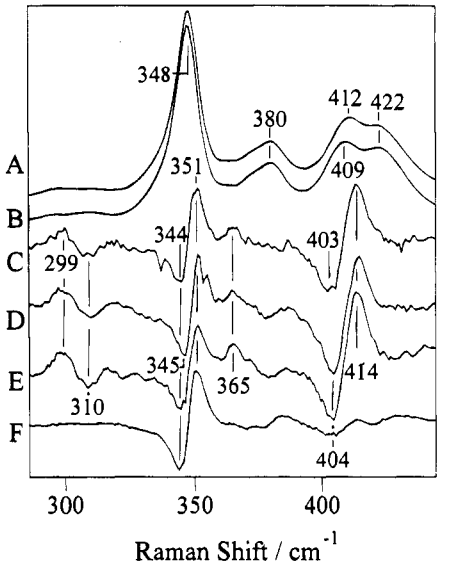

Figure 3. An enlargement showing the low-frequency spectra of the oxygen-bound heme−HO complexes. Each trace is the same as the corresponding trace in Figure 2, except for the enlargement of the *X* and *Y* scales. Trace C is expanded 10 times that of trace A.

the same difference patterns. These results illustrate the independence of the isotope shift pattern on pH, temperature, and D_2O exchange, and hence indicate that all of the features in the difference spectra result from a single unprotonated species. We can thereby exclude the possibility that the spectra result from reaction products such as a coordinated hydroperoxide or an α-hydroxyheme−HO complex. Thus, all of the isotope-sensitive lines originate from the O_2 adduct.

There are several possible origins for the complex shifts we detect. It is necessary to distinguish if the shifts are artifactual, if they originate from small differences in strong porphyrin modes, or if they are real shifts of weak lines. The shifts in the line at 677 cm^{-1} are weak and irreducible (compare traces C, D, and E of Figure 2), and thus are apparently experimental artifacts exaggerated due to the sharpness and intensity of ν_7. These differences are at the limit of our reproducibility. All other major shifts in Figures 2 and 3 are reproducible despite the shift at ν_7. In traces F of Figures 2 and 3, we calculated a derivative of the $^{16}O_2$ spectrum (trace A) by shifting it by 0.25 cm^{-1} to lower frequency and then subtracting it from the original trace. A comparison of this simulated difference spectrum to the experimental difference spectra clarifies several features in the data. First, the large changes we detect in the 565-cm^{-1} line are completely absent from the simulated difference spectrum, confirming our assignment of this line as the ν_{Fe-O_2} mode. In contrast, the experimental shift pattern at 351 cm^{-1} is almost exactly reproduced in the simulated difference spectrum including the asymmetric feature of the shift, strongly suggesting that this shift pattern is caused by a 0.25-cm^{-1} shift to lower frequency of the 348-cm^{-1} porphyrin line (ν_8). The shift in the 412-cm^{-1} region is much larger in the experimental spectra than that in the simulated difference, and it can be identified as a shift of the ~412-cm^{-1} line in the $^{16}O_2$ absolute spectrum to the ~409-cm^{-1} line in the $^{18}O_2$ spectrum (traces A and B of Figure 3). Therefore, we can place limits on this line: the shift of the line must be as large or larger than the 3-cm^{-1} shift detected in the absolute spectra and smaller than the 11-cm^{-1} shift detected in the difference spectrum.[28] In the 1100-cm^{-1} region the differences we detect are most consistent with a small shift (~0.25 cm^{-1}) in the 1134-cm^{-1} line and no shift in the 1122-cm^{-1} line. The weak differences at 299, 310,

(26) Yu, N.-T.; Kerr, E. A. In *Biological Applications of Raman Spectroscopy*; Spiro, T. G., Ed.; Wiley: New York, 1988; Vol. 3, 39−95.
(27) (a) Varotsis, C.; Woodruff, W. H.; Babcock, G. T. *J. Am. Chem. Soc.* **1989**, *111*, 6439−6440. (b) Ogura, T.; Takahashi, S.; Shinzawa-Itoh, K.; Yoshikawa, S.; Kitagawa, T. *J. Am. Chem. Soc.* **1990**, *112*, 5630−5631. (c) Han, S.; Ching, Y.-C.; Rousseau, D. L. *Proc. Natl. Acad. Sci. U.S.A.* **1990**, *87*, 2491−2495.

and 365 cm^{-1} are absent in the simulated spectra and are thereby assigned as real shifts of weak lines in our samples.

In oxyhemoglobin a line at 427 cm^{-1} with an isotope shift of ~21 cm^{-1} has been assigned as the Fe–O–O bending (δ_{Fe-O-O}) mode.[23,24] The line at 412 cm^{-1} in the $^{16}O_2$ adduct of the heme–HO complex could also be assigned to the δ_{Fe-O-O} mode. However, the isotope shift of the line is more than 3 cm^{-1} and less than 11 cm^{-1}, significantly smaller than that of oxyghemoglobin. We could not reproduce such a small isotope shift for a δ_{Fe-O-O} mode by a three-body normal mode calculation with any reasonable choice of force constants, bond lengths, and bending angles. The δ_{Fe-O-O} mode could display an anomalously small isotope frequency shift, if it is coupled to one or more other modes such as those of the porphyrin macrocycle. If we interpret the observed shift pattern at 351 and 414 cm^{-1} as originating from real isotope shifts of weak lines, the sum of the shifts (17 cm^{-1}) is comparable to that of oxyhemoglobin. It is possible to reproduce these shifts by a simple Fermi resonance coupling calculation.[29] However, as discussed above it is more likely that the difference at 351 cm^{-1} is caused by a small shift of the strong ν_8 line rather than a real shift of a weak underlying line. Thus, Fermi resonance coupling of the bending mode with a single porphyrin mode does not appear to be a likely explanation of the data.

As the most consistent explanation of the observed spectra, we assign the unperturbed δ_{Fe-O-O} mode as the line we detect at 412 cm^{-1} in the $^{16}O_2$ adduct but propose that it is strongly coupled with *many* porphyrin modes. Therefore, the isotope shift of the line is much smaller than that of oxyhemoglobin and the shift is distributed over the many porphyrin modes in the 250–400-cm^{-1} range. We interpret the isotope shift at 1138 cm^{-1} as a result of vibrational coupling between heme modes and oxygen modes, but in this region the O–O stretching and the overtone of the ν_{Fe-O_2} modes are expected to appear and are the likely candidates for coupling to the porphyrin modes. Oxygen isotope differences, although different patterns, are also observed in this region of the spectrum for oxymyoglobin and hemoglobin.[24,25]

The low frequency of the ν_{Fe-O_2} mode and the widespread coupling between the modes of the bound-O_2 and porphyrin vibrations are unique features only seen in the heme–HO complex but not in other oxy form of heme proteins. In Figure 4 we plot the normalized isotope shifts of the ν_{Fe-O_2} mode of the oxy forms of the heme–HO complex hemoglobin and myoglobin versus their Fe–O–O bending angles. The bending angles of the latter two proteins were determined crystallographically.[21,30] There is an experimental correlation showing that the smaller the angle, the larger the isotope shift of the ν_{Fe-O_2} mode. This is physically reasonable as may be seen from Figure 5 where the vibrational coordinates for the ν_{Fe-O_2} and δ_{Fe-O-O} modes are depicted. When the Fe–O–O unit is linear the stretching mode may be approximated as a diatomic Fe–O_2 oscillator. However, when the Fe–O–O unit is highly bent,

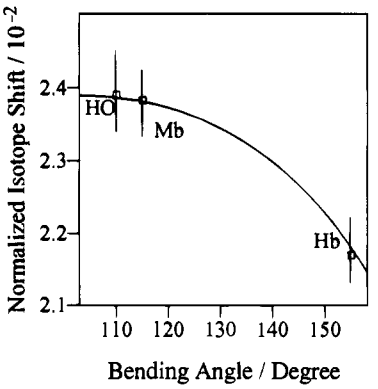

Figure 4. The theoretical isotope shifts expected for the Fe–O_2 stretching mode and the experimental points for hemoglobin (Hb), myoglobin (Mb), and the heme–HO complex (HO). Normalized isotope shifts are defined as follows: (normalized isotope shift) = $[\nu_{(^{16}O_2)} - \nu_{(^{18}O_2)}]/[\nu_{(^{16}O_2)} + \nu_{(^{18}O_2)}]$. The isotope shifts for Hb and Mb were the average of three independent measurements. The bending angles for Hb and Mb are taken from crystallographic data.[20,29] The isotope shift for the HO complex is an average of the readings (accuracy of 0.1 cm^{-1}) for traces C, D, and E of Figure 2. The theoretical curve is based on the three-body (Fe–O–O) normal mode calculation. The details of the calculation are described in the text.

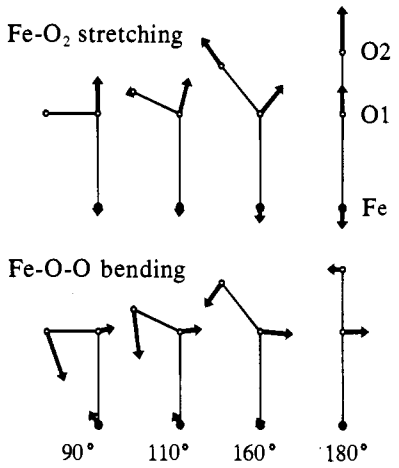

Figure 5. Vector representations of the Fe–O_2 stretching and Fe–O–O bending modes with different bending angles. The calculations were based on the three-body (Fe–O–O) normal mode analysis. The parameters for the calculation were the same as those used in Figure 4.

the mode behaves as an Fe–O oscillator, making the reduced mass of the unit smaller and the isotope shift larger. It is difficult to reproduce this correlation accurately with theoretical calculations, since we do not known how the force constants will change by changing the bending angle. To a first approximation, we can use a set of force constants and bond lengths that can reproduce vibrational data obtained from hemoglobin and change only the Fe–O–O bending angle. The calculated curve is also drawn in Figure 4, which shows that as the Fe–O–O angle approaches 180° the isotope shift becomes smaller. This tendency is independent of the choice of the force constants, as long as the ν_{Fe-O_2} and δ_{Fe-O-O} modes are well separated. Since the oxy form of the heme–HO complex has a slightly larger isotope shift for the ν_{Fe-O_2} mode than that of oxymyoglobin which has a 115° angle, we tentatively estimate the bending angle as ~110°.[30]

The strong vibrational interaction between the bound oxygen and the heme can be understood from this highly bent structure. A calculated space filling model of O_2-bound heme with a 110° bending angle that we propose places the terminal oxygen atom

(28) The apparent shift measured by examination of the absolute spectra is a minimum owing to the overlap with other lines which do not shift upon isotopic substitution. The shift between the peak and the trough in the difference spectrum can be much larger than the true shift of the lines because the separation between the peak and the trough in the difference spectrum reaches a lower limit for small shifts that is given by the derivative of the line shape. As the separation between the lines becomes larger the shift in the difference spectrum approaches the difference between the true positions of the lines. See: Rousseau, D. L. *J. Raman Spectrosc.* **1981**, *10*, 94–99.

(29) (a) Fermi, E. *Z. Phys.* **1931**, *71*, 250–259. (b) Hertzberg, G. In *Molecular Spectra and Structure*; Van Nostrand: New York, 1945; Vol. 2, pp 215–219.

(30) (a) Phillips, S. E. V. *Nature* **1978**, *273*, 247–248. (b) Phillips, S. E. V. *J. Mol. Biol.* **1980**, *142*, 531–554.

in van der Waals contact with a methine bridge carbon atom of the heme plane (if pointing along that direction). The eigenvectors for the δ_{Fe-O-O} mode depicted in Figure 5 show that when the Fe−O−O unit is linear the motion of the terminal oxygen atom (O2 in Figure 5) is parallel to the heme plane. When the Fe−O−O angle is highly bent, not only does the O2 atom come into contact with the heme plane but the motion of the atom has a large contribution perpendicular to the heme plane. The combination of these two effects can induce strong vibrational coupling between the δ_{Fe-O-O} and out-of-plane heme vibrations. In addition, only in the δ_{Fe-O-O} mode with a highly bent structure does the iron have large in-plane movements which can also induce kinematic coupling between the Fe−O−O motion and heme modes. A complete analysis of the vibrational structure requires a full normal coordinate determination of the bent O_2-coordinated porphyrin macrocycle. However, qualitatively, the widespread isotope shifts are interpreted as a consequence of mode coupling between porphyrin modes and modes involving a highly bent Fe−O−O unit.

The small Fe−O−O angle is presumed to be a consequence of direct interactions between the bound O_2 and residues in the distal pocket. We exclude anomalous histidine−Fe coordination as the origin of the unique behavior of the O_2 complex, since the iron−histidine stretching frequency in the deoxy complex (218 cm^{-1})[11-13] is similar to that in myoglobin (220 cm^{-1}).[31] The correlation plot between Fe−CO and CO stretching frequencies of the CO-bound heme proteins is known to be a sensitive probe of the polarity of the proximal ligand.[26,32] The observed point for the heme−HO complex is on the neutral histidine line, confirming the absence of an anomalous trans ligand effect on the bound exogenous ligand.[13] The high-frequency Raman spectrum shows that the electron donation between the bound oxygen and the porphyrin macrocycle is the same as that in oxymyoglobin, indicating a similarity in the electronic states of the porphyrin between the two proteins. All these observations support our interpretation that the effect comes from the unique interaction between distal heme pocket and coordinated oxygen. In a recent magnetic resonance study of the ferric CN bound heme−HO complex, it was suggested that the conformation of the Fe−CN group is also highly bent, consistent with our present interpretation.[33]

The oxygen dissociation rate constant for the oxy form of the heme−HO complex is ~0.01 of that of oxymyoglobin, while the other rate constants such as binding of oxygen and binding and dissociation of CO are of the same magnitude (Ikeda-Saito et al., to be published). The presence of strong interactions between residues in the distal pocket and the bound O_2, inferred from the data reported here, can account for the small dissociation constant of O_2. This ligand discrimination is physiologically important for HO, since otherwise the CO produced by HO would block oxygen binding and subsequent activation. The confinement of the oxygen by the distal residues should also be essential for HO's site specific ring opening, since we hypothesize that it is an α-meso carbon of the porphyrin ring that is in contact with the terminal oxygen atom.

Acknowledgment. This work was supported by NIH Grants Nos. GM39492 and GM48714.

JA942598E

(31) Kitagawa, T.; Nagai, K.; Tsubaki, M. *FEBS Lett.* **1979**, *104*, 376−378.

(32) Uno, T.; Nishinura, Y.; Tsuboi, M.; Makino, R.; Iizuka, T.; Ishimura, Y. *J. Biol. Chem.* **1987**, *262*, 4549−4556.

(33) Hernandez, G.; Wilks, A.; Paolesse, R.; Smith, K. M.; Ortiz de Montellano, P. R.; La Mar, G. N. *Biochemistry* **1994**, *33*, 6631−6641.

(34) The Raman shifts of the ν_{Fe-O_2} modes from Hb, Mb, and the heme-HO complex were estimated both by directly reading the peak and trough positions in the $^{16}O_2$ minus $^{18}O_2$ difference spectra and by fitting the difference spectra by taking differences of Gaussian functions for each of the isotope lines in the absolute spectrum. The agreement between these two methods confirmed that the ν_{Fe-O_2} line widths are sufficiently narrow and the isotope shifts are large enough to allow for direct readings from the difference spectra.